CORA Cork Open Research Archive
Cartlann Taighde Oscailte Chorcaí

Title	Synchrotron maser from weakly magnetized neutron stars as the emission mechanism of fast radio bursts
Authors	Long, Killian;Pe'er, Asaf
Publication date	2018-08-29
Original Citation	Long, K. and Pe'er, A. (2018) 'Synchrotron maser from weakly magnetized neutron stars as the emission mechanism of fast radio bursts', Astrophysical Journal Letters, 864(1), L12 (5pp). doi:10.3847/2041-8213/aada0b
Type of publication	Article (peer-reviewed)
Link to publisher's version	https://iopscience.iop.org/article/10.3847/2041-8213/aada0b/meta - 10.3847/2041-8213/aada0b
Rights	© 2018, the American Astronomical Society. All rights reserved.
Download date	2026-11-16 14:46:23
Item downloaded from	https://hdl.handle.net/10468/7558

UCC
University College Cork, Ireland
Coláiste na hOllscoile Corcaigh

The Astrophysical Journal Letters, 864:L12 (5pp), 2018 September 1 https://doi.org/10.3847/2041-8213/aada0b
© 2018. The American Astronomical Society. All rights reserved.

Synchrotron Maser from Weakly Magnetized Neutron Stars as the Emission Mechanism of Fast Radio Bursts

Killian Long and Asaf Pe'er
Department of Physics, University College Cork, Cork, Ireland; killian.long@umail.ucc.ie
Received 2018 June 7; revised 2018 August 10; accepted 2018 August 11; published 2018 August 29

Abstract

The origin of fast radio bursts (FRBs) is still mysterious. All FRBs to date show extremely high brightness temperatures, requiring a coherent emission mechanism. Using constraints derived from the physics of one of these mechanisms, the synchrotron maser, as well as observations, we show that accretion-induced explosions of neutron stars with surface magnetic fields of $B_* \lesssim 10^{11}$ G are favored as FRB progenitors.

Key words: masers – plasmas – stars: neutron

1. Introduction

Fast radio bursts (FRBs) are bright radio transients of millisecond duration. A total of 33 FRBs have been published to date (Petroff et al. 2016).[1] They have typical fluxes of ∼1 Jy and are distinguished by their large dispersion measures (DMs). These are in the range 176–2596 pc cm^{-3}, an order of magnitude greater than values expected from Milky Way electrons (Champion et al. 2016; Petroff et al. 2016), suggesting an extragalactic origin for FRBs.

Of the 33 FRBs to date, 32 show no evidence of repetition. However, one of the bursts, FRB 121102, has been observed to repeat, allowing it to be localized (Spitler et al. 2016). A persistent counterpart and host galaxy were identified at a redshift of $z = 0.193$, equivalent to a luminosity distance of $d_L = 972$ Mpc, strengthening the case for an extragalactic origin for FRBs (Chatterjee et al. 2017; Marcote et al. 2017; Tendulkar et al. 2017).

The nature of FRB progenitors is still unknown. The small scale and large energies involved has led most models to consider compact objects such as neutron stars to play crucial roles in the production of FRBs. The numerous proposed models fall into two classes, cataclysmic and non-cataclysmic. Cataclysmic models include "blitzars" (collapsing neutron stars; Falcke & Rezzolla 2014), binary neutron star mergers (e.g., Piro 2012), white dwarf mergers (Kashiyama et al. 2013) and neutron star-black hole mergers (Mingarelli et al. 2015). Non-cataclysmic models include giant pulses from extragalactic pulsars and young neutron stars (e.g., Keane et al. 2012; Cordes & Wasserman 2016) and flares from soft gamma repeaters (Popov & Postnov 2013; Lyubarsky 2014; Beloborodov 2017).

Despite the large degree of uncertainty regarding the nature of the progenitor, there is a consensus on the need for a coherent emission process. This follows from the extremely high brightness temperatures of up to $T_b \sim 10^{37}$ K (Katz 2016). As we show here, this requirement holds the key to understanding the nature of the progenitor. Analyzing the conditions required to produce the necessary coherent emission allows us to place strong constraints on possible FRB progenitors.

We find that the conditions found in the environments of neutron stars with surface magnetic fields of $B_* \lesssim 10^{11}$ G are similar to those required for a coherent emission mechanism, the synchrotron maser, to produce an FRB. Furthermore, the proportion of neutron stars with these magnetic fields is ∼10%, and the FRB rate is comparable to this fraction of the neutron star formation rate. These results allow us to propose weakly magnetized neutron stars as being FRB progenitors.

2. The Basic Physics of the Synchrotron Maser

Several mechanisms have been proposed to explain the coherent emission required to produce the extreme brightness temperatures of FRBs. Models include coherent curvature emission (Ghisellini & Locatelli 2018; Kumar et al. 2017), the cyclotron/synchrotron maser (Lyubarsky 2014; Beloborodov 2017; Ghisellini 2017; Waxman 2017), and collisionless Bremsstrahlung in strong plasma turbulence (Romero et al. 2016).

Here we examine the synchrotron maser as the mechanism responsible for FRBs. The maser has the advantage of being a viable emission mechanism over a range of magnetic fields and number densities, as well as not requiring particles to be bunched in small volumes in order to obtain coherent emission (Ghisellini 2017). Previous works invoking the maser have examined specific models (Lyubarsky 2014; Beloborodov 2017; Waxman 2017) or the mechanism itself (Ghisellini 2017), but have not used the mechanism's properties to derive general constraints on the progenitor.

Maser emission is produced due to interaction between electromagnetic waves and energetic particles in a plasma, which can result in negative absorption and stimulated emission under certain conditions (Wu 1985; Treumann 2006). The behavior of the maser is determined by the form of the particle distribution and the environment where it occurs. For masing to occur, a population inversion in the electron distribution is required (Wu 1985; Rybicki & Lightman 1979).

It has been suggested that maser emission occurs in astrophysical sources for two different types of environments, differentiated by whether the plasma magnetization is greater or less than unity, as different mechanisms are responsible in the two cases. The magnetization can be quantified by the ratio ν_p/ν_B, where ν_p is the plasma frequency, given by $\nu_p = \sqrt{ne^2/\pi\gamma m_e}$. Here n is the number density of the plasma, and γ is the Lorentz factor of the electrons. The gyration frequency of the plasma particles, ν_B, is given by $\nu_B = eB/(2\pi\gamma m_e c)$.

[1] http://www.frbcat.org/

Here we examine both cases. In scenario (i) we investigate a homogeneous magnetized plasma ($\nu_p/\nu_B < 1$), with a constant ambient magnetic field B. The plasma consists of a cold background component, which supports the propagation of the waves, and a less dense nonthermal component. The emission is due to gyroresonant interactions between the electrons and electromagnetic waves (Wu 1985). In this scenario, we consider the nonthermal component to be a mildly relativistic magnetized plasma (Louarn et al. 1986), rather than the nonrelativistic magnetized plasma that has been proposed as the source of phenomena such as auroral kilometric radiation (AKR) in Earth's aurora, as well emission from other planets, the Sun, and blazars (Begelman et al. 2005; Treumann 2006). This mechanism is not applicable to highly relativistic plasmas, as masing can only occur when individual harmonics do not overlap (Robinson 1985; Yoon 1990). At higher Lorentz factors, the emission can be described by the synchrotron approximation (e.g., Dulk & Marsh 1982).

In scenario (ii) we consider a weakly magnetized ($\nu_p/\nu_B > 1$) relativistic nonthermal plasma. Maser emission in these conditions has been proposed as the source of radio emission from gamma-ray burst afterglows (Sagiv & Waxman 2002). In this scenario the masing emission is due to the Razin effect, a modification of the emission from a relativistic plasma with respect to the vacuum case, which can result in either suppression or, when a population inversion is present, amplification of the emitted signal (McCray 1966; Zheleznyakov 1967). This is due to a change in the beaming angle of the radiation when the refractive index of the plasma is less than unity (Rybicki & Lightman 1979). For this case, a relativistic plasma is required, as the Razin effect is a relativistic effect and so would not effect cyclotron emission. This restriction does not apply in the magnetized case, due to the Razin effect only being relevant for $\nu_p/\nu_B > 1$, as emission at the Razin frequency of $\nu_{R^*} \approx \nu_p \min\{\gamma, \sqrt{\nu_p/\nu_B}\}$ would otherwise not be visible.

3. Physical and Observational Constraints of the Allowed Parameter Space Region that Enables the Production of FRBs

The physical conditions in the region where the masing takes place can be constrained using the physics of the maser and constraints from observations, allowing us to place limits on the magnetic fields and number densities where the synchrotron maser can plausibly be the emission mechanism for FRBs.

We consider a cataclysmic FRB progenitor. However, as the repeating burst FRB 121102 is the only one to have a known redshift, it is the only source that provides observational constraints for quantities such as the burst energy and the DM of the host galaxy. Therefore, we use the values it provides as representative limits for our calculations.

The data enable us to obtain constraints linking the size and number density of the masing region to the magnetic field of the neutron star. These constraints are obtained from: (i) the energetics of the burst and size of the masing region, (ii) the efficiency of the maser mechanism, (iii) the dispersion measure of the burst, and (iv) the frequency of the signal.

We consider that masing takes place in a spherical shell of thickness d, located a distance R from the central object. The maser will be activated by the formation of a population inversion in the shell. The magnetic fields and short timescale ($\lesssim d/c\Gamma$) required suggest that this object is a neutron star, though the timescale for maser emission is given by the duration of the maser itself (Ghisellini 2017). Assuming that the blast wave is relativistic, the shocked plasma has a width $\sim R/\Gamma$ (Blandford & McKee 1976), where Γ is the Lorentz factor of the blast wave. This typical width provides the first constraint, on the thickness of the shell:

$$d \sim \frac{R}{\Gamma}. \quad (1)$$

The minimum thickness of the shell depends on the number of particles that contribute to the masing, $N_e = E/(\eta\langle E_e\rangle)$, and their number density, n_e. Here, E is the energy of the bursts (in the range 10^{38}–10^{40} erg for the repeater (Law et al. 2017; Tendulkar et al. 2017)), η is the fraction of the electrons' energy that contributes to the maser, and $\langle E_e\rangle$ is the average energy of the masing electrons. These shocked electrons have a thermal energy of $\gamma \approx \Gamma$.

Constraint (ii) originates from the efficiency of the maser. For the maser to be a viable emission mechanism, the growth rate of the signal must be large enough to extract a fraction η of the particle energy. The maser will be quenched when the maser reaches saturation. The efficiency of the maser mechanism in simulations of relativistic shocks was shown to be $\eta \lesssim 10^{-1}$ (e.g., Gallant et al. 1992; Sironi & Spitkovsky 2009). In the case of AKR, the efficiency is in the range $\eta \sim 10^{-1}$–10^{-3} (Wu 1985). The exact value, however, depends on the form of the particle distribution, which is uncertain. We therefore examine values of η in the range $10^{-3} \lesssim \eta \lesssim 10^{-1}$ in this Letter. Lu & Kumar (2018) gave upper limits to the efficiency of $\eta \lesssim 10^{-5}$, derived from limits on the brightness temperature from induced Compton scattering. However, plasma experiments suggest that this saturation effect is not observed for high T_B (Benford & Lesch 1998; Romero et al. 2016).

The growth rate, and therefore the efficiency, depends on the distribution function of the electrons. There is a wide range of possible distributions that can provide the requisite population inversion. We do not specify an exact form for the distribution as our results are unchanged, provided that the growth rate is large enough to extract the required energy over the width of the masing cavity.

The third constraint comes from the dispersion measure. Assuming that the DM from the source is solely due to the particles in the shell, one has $\mathrm{DM_{source}} = \mathrm{DM_{shell}}$, where $\mathrm{DM_{shell}} = n_c d$ for a cold plasma and $\mathrm{DM_{shell}} = n_e d/2\gamma$ for a relativistic plasma. Here, n_c and n_e denote the cold and relativistic electrons in the shell (Shcherbakov 2008). The contribution to the DM from the source region is uncertain. The total DM value also contains contributions from the Milky Way, Milky Way halo, the intergalactic medium and the host galaxy. For FRB 121102, Tendulkar et al. (2017) estimated the DM due to the host galaxy as $55 \lesssim \mathrm{DM_{host}} \lesssim 225\ \mathrm{pc\ cm^{-3}}$. The contribution to this from the galaxy, rather than the source region, depends upon the location of the FRB within the galaxy. Using these values as guidelines, the DM due to the shell is $\mathrm{DM}_{shell} \lesssim 225\ \mathrm{pc\ cm^{-3}}$.

Constraint (iv) is derived from equating the masing frequency to the emission frequency of the bursts, which have observed frequencies of approximately $\nu_{\rm obs} \sim 1.4$ GHz. Here, one discriminates between the two scenarios. For weakly magnetized plasma, the maser frequency is given by the Razin frequency, ν_{R^*}, where the growth rate is at a maximum.

Equating the Razin frequency to the emission frequency of $\nu_{\rm obs}/\Gamma$ and noting $\gamma = \Gamma$ gives the magnetic field in the masing region as

$$B_M = 1.32 \times 10^{-13}\sqrt{n_e^3\gamma^3}. \quad (2)$$

The range

$$1 < \frac{\nu_p}{\nu_B} < \gamma^2 \quad (3)$$

delimits the range where $\nu_{\rm R^*} = \nu_p\sqrt{\nu_p/\nu_B}$. For $\nu_p/\nu_B > \gamma^2$ the Razin frequency is $\nu_{\rm R^*} = \gamma\nu_p$. While masing emission is still possible in this regime, the allowed parameter space is restricted to a small region with low magnetic fields due to constraints from the DM, shell size, and observed emission frequency. Including the neutron stars in this region will not change the statistics for our model discussed below. The range of interest given by Equation (3) can therefore be expressed in terms of the number density using Equation (2) as

$$\frac{2.4 \times 10^{10}}{\gamma^3} < n_e < \frac{2.4 \times 10^{10}}{\gamma}, \quad (4)$$

This provides upper and lower limits on the number density that depend on the Lorentz factor of the electrons.

On the other hand, for the strongly magnetized plasma the frequency of the maser is $\nu_M \approx l\nu_B$, giving a shell magnetic field of

$$B_M \approx 500 l^{-1}\, G. \quad (5)$$

where $\nu_M = \nu_{\rm obs}/\Gamma$ and l is the harmonic number of the fastest growing mode.

4. Results

For both the weakly and strongly magnetized plasmas, we investigate neutron star surface magnetic fields in the range $10^7\,{\rm G} < B_* < 10^{15}\,{\rm G}$. This encompasses the full range of surface magnetic field values for all published pulsars (Manchester et al. 2005).[2] In both cases, the magnetic field outside of the surface was taken to be of the form $B \propto 1/r^3$ inside of the light cylinder, and $B \propto 1/r$ outside (Goldreich & Julian 1969). The light cylinder radius $r_{\rm L} = cP/2\pi$ is the radius at which the co-rotating speed is equal to the speed of light. Here P is the period of the pulsar. We also investigate the full range of number densities in the masing region.

In the weakly magnetized scenario, the range of $n_{\rm e}$ is given by Equation (4). Lorentz factors of $\gamma = 2$, 5, 10, 100, 10^3, and 10^6 were examined. The larger values were chosen to examine conditions similar to pulsar wind nebulae, which have Lorentz factors of up to $\sim 10^6$ (Gaensler & Slane 2006; Kirk et al. 2009). The allowed parameter space for $\gamma = 10$, $E = 10^{40}$ erg, and $\eta = 10^{-3}$ is shown in Figure 1 as an example. In this case, the results indicate that the allowed parameter space is restricted to low magnetic fields and $n \sim 10^8\,{\rm cm^{-3}}$. Increasing the allowed values of the DM results in the lower limit decreasing.

The allowed surface magnetic field values depend on the Lorentz factor, number density in the masing region, and the distance to the masing region, R. As the volume of the shell is $V \approx 4\pi R^2 d$, the distance to the masing region and the number density are related by the expression

$$R \approx \left(\frac{E}{4\pi\eta mc^2 n_e}\right)^{1/3}. \quad (6)$$

Using Equation (2), the surface magnetic field can therefore be expressed as $B_* \propto n_e^{7/6}\gamma^{3/2}$. Taking into account the maximum allowed number density from Equation (4), $n_{e,\rm max} \propto \gamma^{-1}$, the maximum surface magnetic field is $B_{*,\rm max} \propto \gamma^{1/3}$. Thus, the allowed surface magnetic field depends only weakly on the Lorentz factor. Therefore, even for very large values of γ only low values of B_* are attainable.

We find that a neutron star with a surface magnetic field of $B_* \lesssim 10^{10}$–$10^{11}\,{\rm G}$ is required for emission at the appropriate frequency and energy, increasing to $B_* \lesssim 10^{12}\,{\rm G}$ only in the extremely relativistic $\gamma = 10^6$ case. Ruling out pulsars with magnetic fields greater than $10^{11}\,{\rm G}$ leaves approximately 14.5% of the total population (Manchester et al. 2005). For FRBs with lower energy and greater efficiency, the upper limit on the magnetic field can be significantly lower at $\sim 10^{9.5}\,{\rm G}$. Less than 10% of pulsars have magnetic fields lower than this value. These upper limits on B_* are thus very strong constraints, as they rule out the majority of pulsars as being possible hosts for the synchrotron maser in the context of FRBs. The ~15% of the known pulsar population that meet the criteria are therefore candidates for FRB progenitors. Therefore, the FRB rate should be a similar fraction of the neutron star formation rate. The neutron star formation rate is approximated by the core-collapse supernova rate that is approximately $\mathcal{R}_{\rm SN} \sim (1.42 \pm 0.3) \times 10^5\,{\rm Gpc^{-3}\,yr^{-1}}$ (Bazin et al. 2009), while the rate of FRBs is approximately $\mathcal{R}_{\rm FRB} \sim 0.98^{+1.15}_{-0.89} \times 10^4\,{\rm Gpc^{-3}\,yr^{-1}}$ (Champion et al. 2016). The ratio of the two rates is $\mathcal{R}_{\rm FRB}/\mathcal{R}_{\rm SN} \sim 0.07$. This value is similar to the fraction of pulsars with surface magnetic fields of less than $10^{10}\,{\rm G}$, which is ~0.1.

The limits obtained from $\rm DM_{shell}$ also constrain our results significantly. They have a particularly marked effect in the cases with larger numbers of particles in the masing region. For the higher energy bursts, the DM limits severely constrain the cases with lower Lorentz factors, while for the lower energy bursts they are only relevant for $\Gamma = 2$. The lower limit on n_e depends on the case under consideration. Bursts with higher

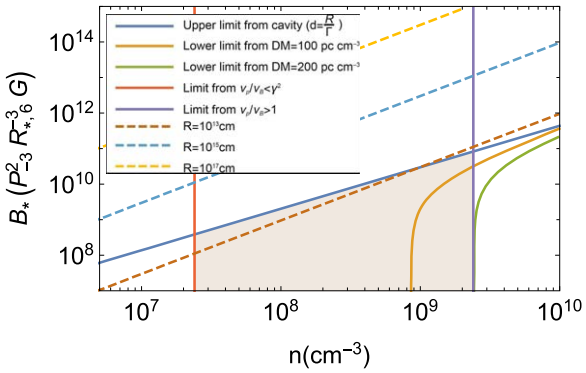


Figure 1. Parameter space (shaded region) for the synchrotron maser with $\nu_p/\nu_B > 1$, $\gamma = 10$, $E = 10^{40}$ erg and $\eta = 10^{-3}$. The solid lines show limits, while the dashed lines show lines of constant radius. Values of $B_* \lesssim 10^{10}$ G, $n \sim 10^8\,{\rm cm^{-3}}$, and $R \sim 10^{13}$ cm are preferred. For larger DM values the lower limit will decrease. Increasing the value of γ results in less-restrictive DM constraints, lower allowed number densities and higher allowed neutron star surface magnetic field values.

[2] http://www.atnf.csiro.au/research/pulsar/psrcat

energies and Lorentz factors have lower allowed number densities. The lowest density of $\sim 1\,\mathrm{cm}^{-3}$ was achieved for $\gamma = 10^6$.

For the highly magnetized plasma scenario, we examine background (cold electron) number densities of up to $n_c = 10^7\,\mathrm{cm}^{-3}$, as values larger than this were ruled out by constraints from the DM. For each value of n_c, we examine the range $10^{-3} < \frac{n_e}{n_c} < 10^{-1}$, where the lower limit is set by the luminosity requirements. The growth rate decreases with n_e, and so smaller values result in growth rates that are too low to produce the required luminosity. A Lorentz factors of $\gamma = 2$ was examined, as the maser in this case is not relevant in highly relativistic scenarios. At the maximum number density of $n_c \sim 10^7\,\mathrm{cm}^{-3}$, the upper limit on the surface magnetic field is $\sim 10^{12}$ G. As $B_* \propto n^{-1/3}$; at low number densities, higher magnetic fields are obtainable. However, this scenario can be ruled out entirely through constraints obtained from the physics of the blast wave.

The Lorentz factor of a blast wave expanding into the interstellar medium (ISM) is given by

$$\Gamma = \left(\frac{17E}{16\pi n_{\rm ISM} m_p c^2 R^3}\right)^{1/2}, \tag{7}$$

where E is the energy of the blast wave, m_p is the proton mass, $n_{\rm ISM}$ is the density of the ISM and $n_e \ll n_c$ (Blandford & McKee 1976). This gives the distance to the shell as $R_{15} \lesssim 1.31 E_{40}^{1/3} n_{\rm ISM,0}^{-1/3} \eta_{-3}^{-1/3} \Gamma_0^{-2/3}$ cm, where $Q = 10^x Q_x$ in cgs units. Using Equation (5) and $B_* \approx \frac{c^2 P^2 B_M R}{4\pi^2 R_*^3}$, this condition restricts the surface magnetic field to

$$B_{*,13} \lesssim 1.49 E_{40}^{1/3} n_{\rm ISM,0}^{-1/3} \eta_{-3}^{-1/3} \Gamma_0^{-2/3} R_{*,6}^{-3} P_{-3}^{2} l^{-1}\ \mathrm{G}\ . \tag{8}$$

Here, R_* is the radius of the neutron star. However, the number density is also related to R and B_* through Equation (1), resulting in the condition

$$B_{*,13} \approx 11.3 E_{40}^{1/3} n_{\rm ISM,0}^{-1/3} \eta_{-3}^{-1/3} R_{*,6}^{-3} P_{-3}^{2} l^{-1}\ \mathrm{G}. \tag{9}$$

Equation (9) does not satisfy the condition in Equation (8) for any value of Γ. Therefore, the maser in a strongly magnetized plasma can be ruled out as the possible emission mechanism.

5. Discussion

Emission from the synchrotron maser can be circularly, elliptically, or approximately linearly polarized, depending on the electron distribution function and plasma parameters (Sagiv & Waxman 2002; Treumann 2006). Similarly, both circular (e.g., Masui et al. 2015) and linear polarization (e.g., Michilli et al. 2018) has been measured in FRB observations. However, the heterogeneous nature of FRB polarization measurements to date makes it difficult to draw useful constraints from the data.

The density constraints obtained from the maser can be compared to the densities found in the vicinity of neutron stars. In the case of pulsar wind nebulae, densities of $n \sim 10^{-6}\,\mathrm{cm}^{-3}$ and magnetic fields of $B_M \sim 10^{-2} - 10^{-1}$ G are expected (Gaensler & Slane 2006; Kirk et al. 2009; Lyubarsky 2014; Olmi et al. 2014). Neither of these values lie within the allowed parameter space for the synchrotron maser, ruling out this scenario.

In order to account for the larger density values required by our constraints, we are led to suggest a scenario where weakly magnetized neutron stars undergo an accretion-induced explosion (Katz et al. 1994). The material expelled by this explosion can then form a shell of width $\sim R/\Gamma$ in which a population inversion is formed, and as a result masing takes place. Accreting neutron stars in low mass X-ray binaries have typical wind densities of 10^{13}–$10^{15}\,\mathrm{cm}^{-3}$ at radii of approximately 10^{10} cm (Díaz Trigo & Boirin 2016). While these density values are too high for the maser, our scenario considers the masing emission to occur at larger distances of $R \sim 10^{13}$ cm. As at constant velocity $n \propto r^{-2}$, the particles from the accretion-induced explosion could plausibly provide suitable number densities for the maser at these distances. Pulsars in binary systems with $B_* < 10^{11}$ G have typical periods of $\sim$few ms and make up $\sim$0.09 of the total population (Manchester et al. 2005), comparable to the ratio of the FRB and neutron star formation rates. As a result, this scenario would require a significant fraction of low magnetic field neutron stars in binaries to undergo such an event due to the similarities between the FRB rate and the neutron star formation rate. The scenario where the masing occurs in a strongly magnetized plasma is ruled out due to the impossibility of obtaining a blast wave of sufficient velocity at the required radius and number density.

K.L. acknowledges the support of the Irish Research Council through grant number GOIPG/2017/1146. The authors also thank the referee for useful comments.

ORCID iDs

Killian Long https://orcid.org/0000-0003-1215-9003
Asaf Pe'er https://orcid.org/0000-0001-8667-0889

References

Bazin, G., Palanque-Delabrouille, N., Rich, J., et al. 2009, A&A, 499, 653
Begelman, M. C., Ergun, R. E., & Rees, M. J. 2005, ApJ, 625, 51
Beloborodov, A. M. 2017, ApJL, 843, L26
Benford, G., & Lesch, H. 1998, MNRAS, 301, 414
Blandford, R. D., & McKee, C. F. 1976, PhFl, 19, 1130
Champion, D. J., Petroff, E., Kramer, M., et al. 2016, MNRAS, 460, L30
Chatterjee, S., Law, C. J., Wharton, R. S., et al. 2017, Natur, 541, 58
Cordes, J. M., & Wasserman, I. 2016, MNRAS, 457, 232
Díaz Trigo, M., & Boirin, L. 2016, AN, 337, 368
Dulk, G. A., & Marsh, K. A. 1982, ApJ, 259, 350
Falcke, H., & Rezzolla, L. 2014, A&A, 562, A137
Gaensler, B. M., & Slane, P. O. 2006, ARA&A, 44, 17
Gallant, Y. A., Hoshino, M., Langdon, A. B., Arons, J., & Max, C. E. 1992, ApJ, 391, 73
Ghisellini, G. 2017, MNRAS, 465, L30
Ghisellini, G., & Locatelli, N. 2018, A&A, 613, A61
Goldreich, P., & Julian, W. H. 1969, ApJ, 157, 869
Kashiyama, K., Ioka, K., & Mészáros, P. 2013, ApJL, 776, L39
Katz, J. I. 2016, MPLA, 31, 1630013
Katz, J. I., Toole, H. A., & Unruh, S. H. 1994, ApJ, 437, 727
Keane, E. F., Stappers, B. W., Kramer, M., & Lyne, A. G. 2012, MNRAS, 425, L71
Kirk, J. G., Lyubarsky, Y., & Petri, J. 2009, ASSL, 357, 421
Kumar, P., Lu, W., & Bhattacharya, M. 2017, MNRAS, 468, 2726
Law, C. J., Abruzzo, M. W., Bassa, C. G., et al. 2017, ApJ, 850, 76
Louarn, P., Le Queau, D., & Roux, A. 1986, A&A, 165, 211
Lu, W., & Kumar, P. 2018, MNRAS, 477, 2470
Lyubarsky, Y. 2014, MNRAS, 442, L9
Manchester, R. N., Hobbs, G. B., Teoh, A., & Hobbs, M. 2005, AJ, 129, 1993
Marcote, B., Paragi, Z., Hessels, J. W. T., et al. 2017, ApJL, 834, L8
Masui, K., Lin, H.-H., Sievers, J., et al. 2015, Natur, 528, 523
McCray, R. 1966, Sci, 154, 1320
Michilli, D., Seymour, A., Hessels, J. W. T., et al. 2018, Natur, 553, 182
Mingarelli, C. M. F., Levin, J., & Lazio, T. J. W. 2015, ApJL, 814, L20
Olmi, B., Del Zanna, L., Amato, E., Bandiera, R., & Bucciantini, N. 2014, MNRAS, 438, 1518
Petroff, E., Barr, E. D., Jameson, A., et al. 2016, PASA, 33, e045

Piro, A. L. 2012, ApJ, 755, 80
Popov, S. B., & Postnov, K. A. 2013, arXiv:1307.4924
Robinson, P. A. 1985, PPCF, 27, 1037
Romero, G. E., del Valle, M. V., & Vieyro, F. L. 2016, PhRvD, 93, 023001
Rybicki, G. B., & Lightman, A. P. 1979, Radiative Processes in Astrophysics (New York: Wiley)
Sagiv, A., & Waxman, E. 2002, ApJ, 574, 861
Shcherbakov, R. V. 2008, ApJ, 688, 695
Sironi, L., & Spitkovsky, A. 2009, ApJ, 698, 1523
Spitler, L. G., Scholz, P., Hessels, J. W. T., et al. 2016, Natur, 531, 202
Tendulkar, S. P., Bassa, C. G., Cordes, J. M., et al. 2017, ApJL, 834, L7
Treumann, R. A. 2006, A&ARv, 13, 229
Waxman, E. 2017, ApJ, 842, 34
Wu, C. S. 1985, SSRv, 41, 215
Yoon, P. H. 1990, PhFlB, 2, 867
Zheleznyakov, V. V. 1967, SvA, 11, 33